iScience

Article

Increased brightness assimilation in rod vision

Graphical abstract

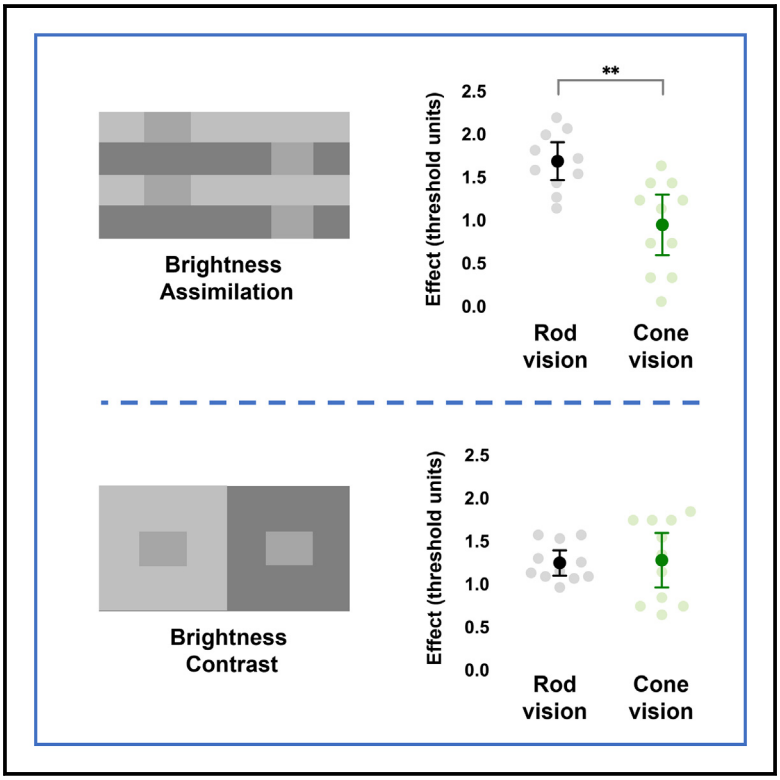

Authors

Pablo A. Barrionuevo, Alexander C. Schütz, Karl R. Gegenfurtner

Correspondence

pbarrionuevo@herrera.unt.edu.ar

In brief

Sensory neuroscience; Cognitive neuroscience

Highlights

- Rod vision enhances brightness assimilation but not brightness contrast
- Transparency is underestimated at low light levels
- Rod-mediated brightness assimilation relies more on inferences than cone vision

Barrionuevo et al., 2025, iScience *28*, 111609
February 21, 2025
https://doi.org/10.1016/j.isci.2024.111609

CellPress

iScience

CellPress
OPEN ACCESS

Article

Increased brightness assimilation in rod vision

Pablo A. Barrionuevo,[1,2,4,*] Alexander C. Schütz,[3] and Karl R. Gegenfurtner[1]
[1]Allgemeine Psychologie, Justus-Liebig-Universität, Giessen, 35394 Hessen, Germany
[2]Instituto de Investigación en Luz, Ambiente y Visión, Consejo Nacional de Investigaciones Científicas y Técnicas – Universidad Nacional de Tucumán, San Miguel de Tucumán, Tucumán T4002BLR, Argentina
[3]Allgemeine und Biologische Psychologie, Philipps-Universität Marburg, Marburg, 35032 Hessen, Germany
[4]Lead contact
*Correspondence: pbarrionuevo@herrera.unt.edu.ar
https://doi.org/10.1016/j.isci.2024.111609

SUMMARY

Our visual system uses contextual cues to estimate the brightness of surfaces: brightness can shift toward (assimilation) or away from (contrast) the brightness of the surroundings. We investigated brightness induction at different light levels and found a potential influence of rod photoreceptors on brightness induction. We then used a novel tetrachromatic display to generate stimuli differentially exciting rods or cones at a fixed light adaptation level. Under rod vision, brightness assimilation was enhanced while brightness contrast was not altered in comparison to cone vision. We ruled out that this effect was mediated by the low resolution of night vision. Our findings suggest that rod vision affects the high-level interpretation of visual scenes that results in differences in brightness assimilation but not contrast. Our results imply that the visual system employs more perceptual inferences under rod vision than under cone vision to solve visual ambiguities in complex spatial displays.

INTRODUCTION

To estimate the brightness of a surface, the human visual system uses contextual cues to resolve the ambiguity that a given luminance can result from an infinite number of combinations of illuminations and surface reflectances. The inference of an object's reflectance is possibly one of the most preserved perceptual functions throughout evolution since it can provide useful information about the edibility and harmfulness of objects, and therefore can be crucial for survival.

In a visual scene with dark and bright surfaces, gray patches are perceived as brighter or darker depending on the geometry and regularity of the surrounding surfaces. When the patches' brightness becomes more similar to the surrounding brightness (Figure 1A), the induction is called assimilation. Another type of induction is brightness contrast, where the patches' brightness shifts "away" from the surrounding brightness (Figure 1A).

It is well known that brightness perception is a multistage process, involving retinal, subcortical, and cortical areas.[6] Brightness induction has been vastly studied using computer monitors with photopic light adaptation and foveal viewing, i.e., in conditions that favor cone photoreceptors.[6–8] At lower light levels such as those occurring naturally at dawn and dusk, rod photoreceptors contribute to contrast perception.[9–11] Furthermore, night (scotopic) vision is only mediated by rods, since cones are insensitive at low light levels.[12]

Rod vision differs from cone vision in many physiological and perceptual aspects. Rods are absent in the fovea; they have a partially exclusive pathway only at the retinal level[9] and the rod pathway shows larger spatial and temporal integration than the cone pathway. These differences have important perceptual consequences. For example, motion perception is affected when seen by rods[13]; a piece of paper perceived as white in photopic levels is perceived as gray in almost darkness[14]; hue can be affected when rods are involved,[15,16] and central vision is preferred even below cone thresholds.[17]

Since rod responses signal light increments,[18] the brightness estimation in scotopic conditions is entirely driven by rods.[19,20] For simple background test spatial configuration, local adaptation can account for cone-driven brightness matching,[21] but it cannot explain rod-driven brightness matching[22] which was better explained by a neural spatial reorganization hypothesis.[23] Classical studies about rod-driven brightness perception focused on the interaction with cones using stimuli with different spectral compositions and light levels that favor rods or cones.[24–26] Regarding rod-driven brightness induction, previous studies found contradictory results. On the one hand, it was reported that contrast and assimilation at scotopic light levels were preserved.[27,28] On the other hand, another type of brightness contrast (the grating induction) was found to disappear at scotopic light levels.[29] However, these previous studies did not provide a fair comparison of rod and cone vision. A fair comparison between rod and cone vision requires testing at the same light adaptation regimes.[9] This requirement can be achieved by the silent substitution method in novel multi-primary displays,[30–34] which allows customization of complex spatiotemporal stimulation for individual photoreceptor types at the same background light adaptation.[35,36] To our knowledge, just one previous study using a two-branch optical device for silent substitution has reported brightness contrast induced by rod excitation.[37] However, this study was unsuccessful in finding a nulling condition in high mesopic light levels (10 and 100td),

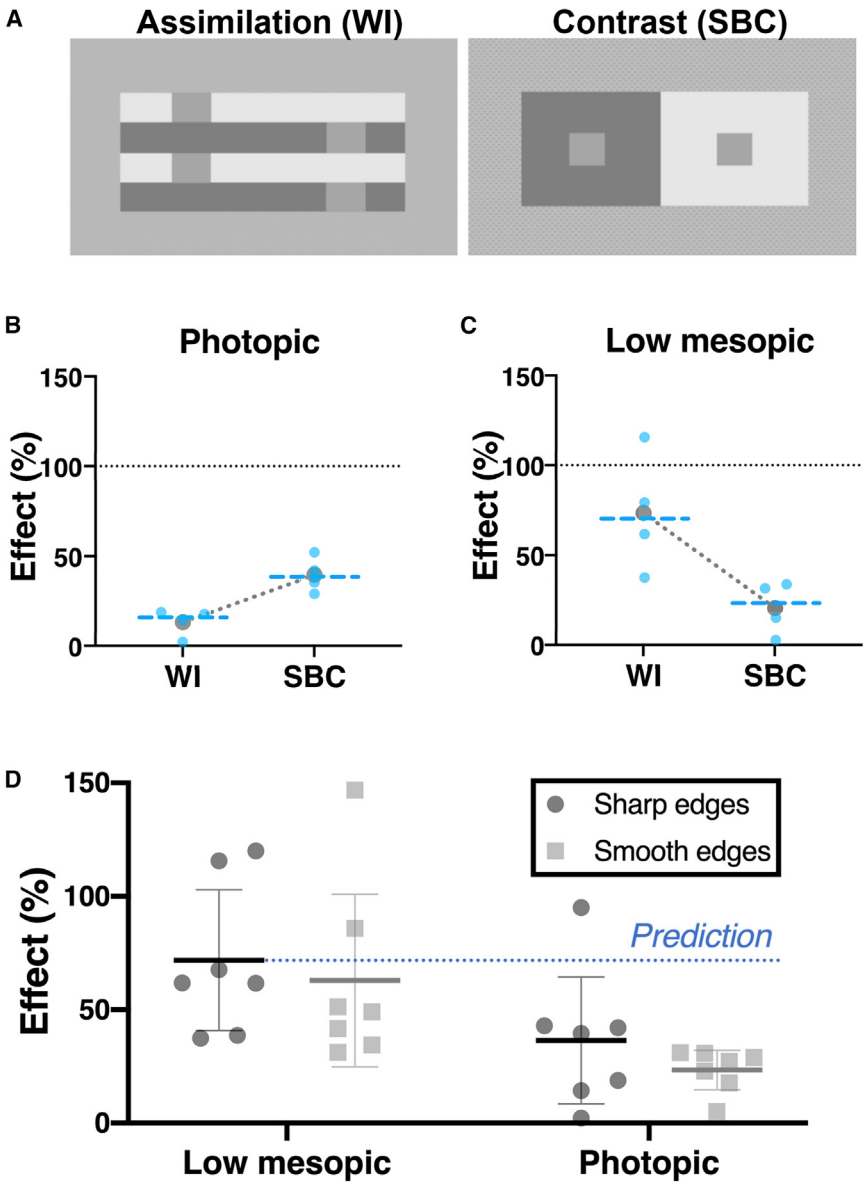

Figure 1. The effect of light level on brightness induction

(A) The stimuli of brightness induction for assimilation and contrast used in this work were the White's illusion[1] (WI), and the simultaneous brightness contrast[2] (SBC), respectively.

(B and C) Results of Experiment 1.1. Brightness induction (percentual effect) for brightness assimilation (WI) and contrast (SBC) at two adaptation light levels with different participation of cones and rods[3]; photopic (higher participation of cones than rods[4,5]), (B) and low mesopic (higher participation of rods than cones, (C) conditions. Light blue circles represent individual data, gray circles represent the mean values, and light blue dashed lines represent median values. Although the effect for photopic WI (B) appears small, it was significantly larger than zero ($t(3) = 3.48$, $p = 0.04$).

(D) Results of Experiment 1.2. The brightness assimilation effect was lower at photopic than at low mesopic conditions for both sharp and smooth edges. Markers represent individual data for sharp (dark gray circles) and smooth (light gray squares) edges. Horizontal wide lines represent mean and error bars represent 95% confidence intervals. Effects equal to zero mean no induction. See also Figures S1, S2, S5, and S6.

thus there was no possible comparison between rod and cone-driven induction, probably due to different temporal response functions of rod and cone processing and/or the influence of cones to multiple post-receptor pathways.

Since the first reports of the importance of surface boundaries and contrast on the estimation of brightness, more than 150 years have passed.[2,38] However, this induction effect was traditionally assessed for cone-vision. The estimation of surface reflectance is greatly affected in rod vision[14] and rod vision is characterized by much lower spatial resolution,[11] therefore, we investigated how contextual cues are used to estimate brightness when rods are involved. Using a tetrachromatic display, we generated stimuli exciting rods, and/or cones at the same light adaptation level. We found that under rod vision brightness assimilation was enhanced while brightness contrast was not altered in comparison to cone vision, and this effect was not mediated by the low resolution of rod vision. Our results suggest that low-level retinal processing differences between rods and cones have an important impact on the high-level interpretation of the brightness in a visual scene.

RESULTS

Experiment 1.1. Testing the effect of light level

In this first experiment, we studied the effect of light adaptation on brightness induction. The idea here was that different relative contribution of rods and cones can provide a first clue about the role of these photoreceptor in brightness induction. We produced two different background light levels for light adaptation purposes using a regular monitor and neutral density filter. These levels were photopic (55.3 cd/m^2) and low mesopic (0.014 cd/m^2). After light adaptation to the background, participants had to choose the brighter patch between the gray patches embedded in the inducing configurations (Figure 1A). The inducers were horizontal bars in the White's illusion (WI) and big rectangles in the simultaneous brightness contrast (SBC). The patches could have a reference value or a variable value. For the SBC, the gray patch in the center of the left inducer (dark background in Figure 1A) had to be compared with the gray patch at the center of the right inducer (bright background in Figure 1A). For the WI, the two gray rectangles at the left had to be

compared with the two at the right. Following a constant-stimuli procedure, we quantified the effect of the induction as the difference between the point of subjective equality (PSE) and the reference luminance, divided by the reference luminance. The PSE was the luminance of the test patch at which participants rated its brightness as higher than the reference patch brightness at a probability of 50%. To make both effects (assimilation and contrast) comparable in magnitude, we report their absolute values.

The results of this experiment are shown in Figures 1B and 1C. We found significant differences corresponding to the light level ($F(1,6) = 7.602$, $p = 0.033$), but not with respect to the induction type ($F(1,6) = 0.4618$, $p = 0.5221$). An interaction between light level and induction type was also found ($F(1, 6) = 9.596$, $p = 0.0212$). Interestingly, the effect of the WI induction was significantly lower for the photopic level in comparison to the low mesopic level (Sidak's: $p = 0.0051$), however the effect of the SBC stimulus at the two adaptation conditions was not different ($p = 0.4302$).

Experiment 1.2. Testing the "poor resolution at low-light levels" hypothesis

One potential explanation for the results of Experiment 1.1 is related to the poorer spatial resolution at low light levels, which is characteristic of rod vision.[39] This could lead to a blurring of the stimulus, which would act in a manner similar to assimilation. We therefore performed a control experiment using a smoothed stimulus (without high-spatial frequency components). If this stimulus would have a similar effect than the sharp-edge stimulus at low mesopic levels, we can rule out this possibility. We used the same psychophysical methodology as in Experiment 1.1. We found a similar effect with and without smoothing in both photopic and low mesopic light levels, with a lower effect in photopic levels as expected from Experiment 1.1 ($F(1, 6) = 11.13$, $p < 0.0157$). A significant difference between the photopic sharp-edge and low mesopic smooth-edge conditions (Tukey's: $p = 0.0206$) was also found, Therefore, we can reject poorer spatial resolution in the rod system as an explanation for the differences observed (Figure 1D). We address the potential role of high spatial frequencies in detail in the supplemental information (Figures S1 and S2).

Since changes in resolution were ruled out as possible explanation, the discrepancies in our results for the different light levels might be related to different perceptual effects of rod and cone signals. An elegant way to test this possibility is to generate selective stimulation of rods and cones at the same light adaptation condition.

The contribution of photoreceptor types

In a second set of experiments we used a display with four primaries (tetrachromatic display) to generate isolation of photoreceptor excitations through the application of the silent substitution method at the pixel level[35] (Figures 2A–2C). With this method, we produced different visual conditions (Figures 2D–2G): Rod vision (exclusive differential excitation of rods), Cone vision (exclusive and simultaneous excitation of the S, M, and L cones), and LMSR (combined rod and cone vision). All stimuli had the same background adaptation level (1.92 cd/m^2). For further explanation of this method see the supplemental information (Figure S3. Calibration to apply silent substitution). For each visual condition, we generated two inducing configurations: (1) "Assimilation" based on the White's illusion and (2) "Contrast" based on the simultaneous brightness contrast illusion (Figure 1A).

The position of the inducers (horizontal bars in WI and big rectangles in SBC) was randomly toggled. The patches could have a reference value or a variable (test) value. Reference and test positions were randomly interchanged between left and right positions. For the SBC, the gray patch in the center of the left inducer had to be compared with the gray patch at the center of the right inducer. For the WI, the two gray rectangles at the left had to be compared with the two at the right. After light adaptation to the background, participants had to choose the brighter patch between two patches embedded in the inducing configurations. Since rod-inducing and cone-inducing brightness can be canceled by the respective physical patch excitation modulation,[37,40] the rod and/or cone test patch excitation was changed following an adaptive procedure.

The stimuli were presented monocularly and extra-foveally. Through a gaze-contingency paradigm,[41] we controlled that the participants were not able to perceive the stimulus foveally. See STAR Methods section for further details.

Experiment 2.1. Maximum stimulus contrasts

In this experiment, the inducer contrasts were set at the maximum values allowed by the gamut of the experimental condition (Rod vision: 42%, Cone vision: 30%, LMSR: 100%). Results are shown in Figure 3. For rod vision (Figure 3A), the induction effect was higher for assimilation (WI, mean ± s.d.: 0.79 ± 0.19) than for contrast (SBC, Mean ± s.d.: 0.48 ± 0.18) and this difference was significant ($t(9) = 4.53$, $p = 0.0014$). For cone vision (Figure 3B), the trend was opposite with a higher value for contrast (mean ± s.d.: 0.57 ± 0.23) than for assimilation (mean ± s.d.: 0.5 ± 0.21), however, these effects didn't significantly differentiate ($t(9) = 1.025$, $p = 0.33$). For the combined rod-cone vision (LMSR, Figure 3C), the effect for contrast (mean ± s.d.: 0.36 ± 0.29) was higher than for assimilation (mean ± s.d.: 0.25 ± 0.12), however, both inductions didn't show significant differences ($t(9) = 1.93$, $p = 0.086$). These results mimicked the increase of assimilation with decreasing light levels from photopic to scotopic viewing conditions found in Experiment 1.1 (Figures 1B and 1C). From this experiment, we still cannot directly compare rod and cone vision for the same type of induction because stimulus contrasts differed between the photoreceptors. Therefore, we equalized the stimulation for each photoreceptor condition in the following experiment.

Experiment 2.2 Estimation of contrast thresholds

To be able to compare the strength of each induction between rod vision and cone vision, we obtained contrast thresholds for all stimulus conditions (Figure 4). We measured the contrast threshold for rod vision, cone vision (LMS), and combined rods and cones (LMSR). The stimulus was presented extra-foveally (inset of Figure 4A). The participants had to choose the vertical bar in each trial, and the stimulus contrast modified across trials following an adaptive procedure to obtain the discrimination

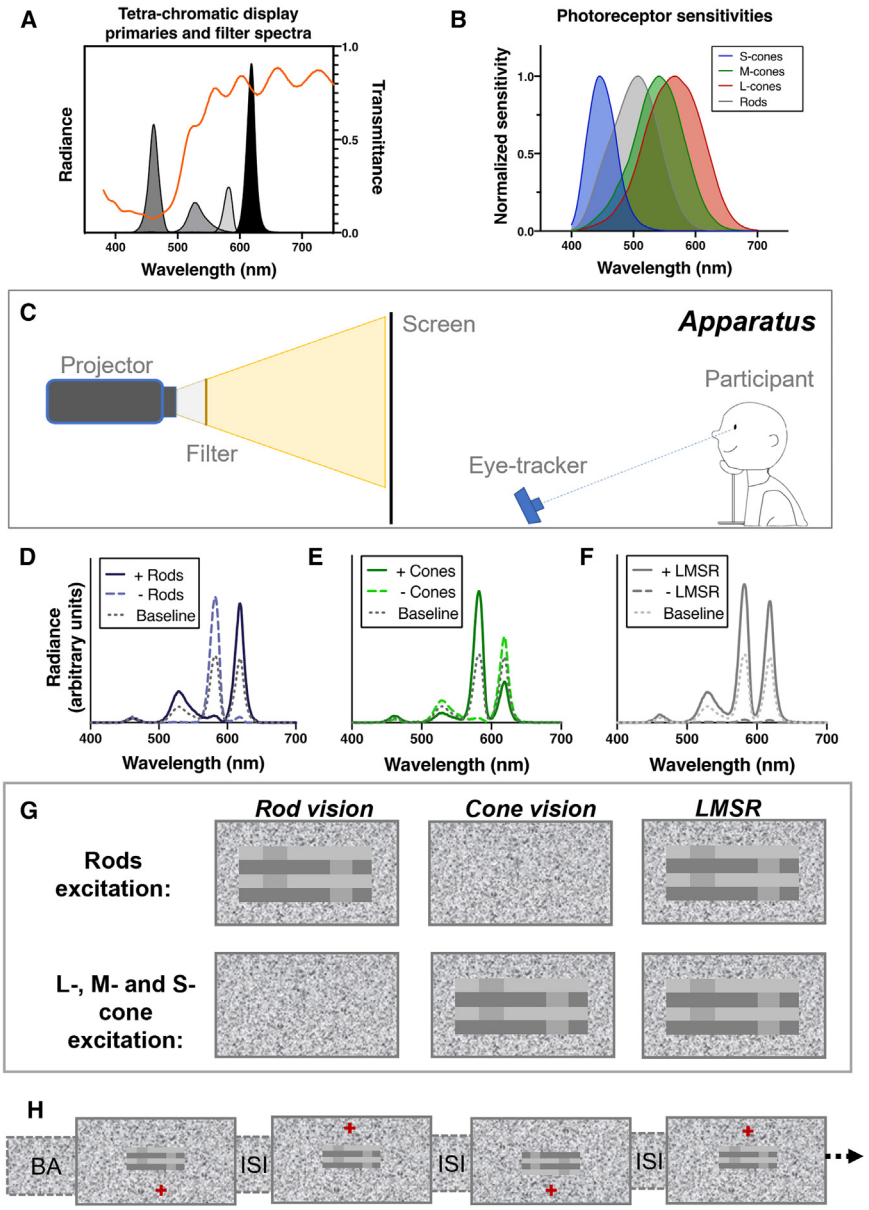

Figure 2. Methodological considerations to achieve isolation of rod and cone vision and quantify brightness induction

(A) The spectral radiance profile of the projector primaries and transmittance of the optical filter that covers the projector output.

(B) the normalized photoreceptor sensitivities at the corneal level.

(C) Schematic representation of the apparatus used for conducting the experiments 2.1–2.3.

(D–F) Spectra of the primaries after filtering (through a yellow filter) and application of silent substitution method to isolate rods (D), cones (E) or for the combined rod and cone condition (LMSR, F) for contrast increment (solid lines), contrast decrement (dashed lines), and baseline (point lines).

(G) Representation of the photoreceptor excitations for each visual condition (Rod vision, Cone vision, and LMSR).

(H) Temporal procedure for Experiments 2.1 and 2.3, including the initial background adaptation (BA) and the interstimulus interval (ISI). The fixation cross was alternatively toggled between up and down, while the inducer's position was randomly changed across trials. See also Figures S3 and S4.

threshold. To avoid any change on the threshold due to background chromaticity dependence,[31,42,43] the stimuli were presented at the same chromaticity as the background for the main experiment. Our results showed mean contrast thresholds of 19% for rods, 4% for cones, and 5% for LMSR (Figure 4). Due to the large difference between rod and cone contrast thresholds, we used the contrast thresholds of this experiment to produce a fair comparison of rod and cone vision when testing brightness induction.

Experiment 2.3. Normalization by threshold units

The comparison of rod and cone vision was conducted by matching the stimuli in terms of threshold units (see Figures 4B–4D and STAR Methods section). Inducing stimuli excitations were set, such that they provided the same stimulation for rods and cones, based on matching threshold units (TU) for both types of photoreceptors obtained in Experiment 2.2. The inducing effect was computed as the TU difference between a reference patch (with a constant excitation) and the test patch excitation needed to match them in brightness.

As expected from the previous experiments, results from this experiment show again that for rod vision (Figure 5A), the induction effect for assimilation (WI in TU, mean ± s.d.: 1.7 ± 0.33) was higher than the effect for contrast (SBC in TU, mean ± s.d.: 1.3 ± 0.22), and this difference was significant ($t(10)$ = 4.67, p = 0.0009). While for cone vision (Figure 5B), the induction effect for contrast (TU, mean ± s.d.: 1.3 ± 0.47) was higher than for assimilation (TU, mean ± s.d.: 0.95 ± 0.53), however, there was no significant difference between both induction types ($t(10)$ = 1.455, p = 0.1763). These effects were similar to those found in experiment 2.1. In the LMSR condition (Figure 5C), the differences between assimilation and contrasts were not significant (TU, mean ± s.d.: 1.2 ± 0.39 (WI) vs. 1.1 ± 0.51 (SBC); $t(10)$ = 0.7861, p = 0.45). Note that due to the normalization procedure based on TU, the LMSR of Experiment 2.3 contains a rod stimulation below the rod contrast threshold found in Experiment 2.2. In this way this condition differs from the LMSR condition of Experiment 2.1.

With these experimental conditions we can directly compare rod and cone vision for the same induction type (Figures 5D–5F). We found that rod vision produced higher assimilation

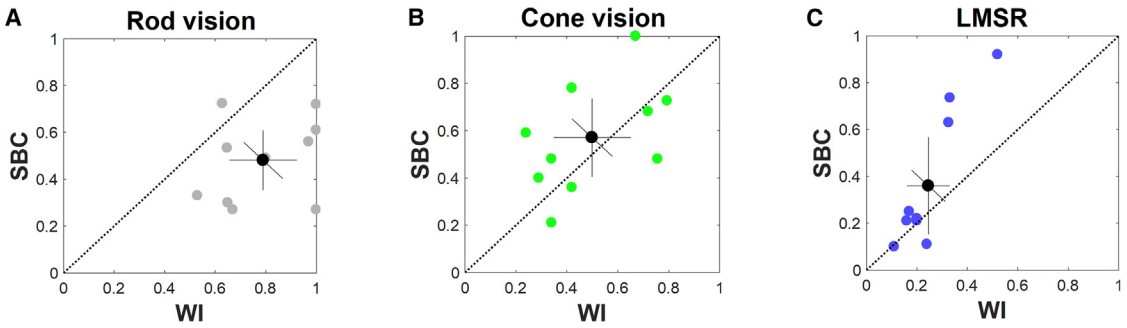

Figure 3. Brightness induction for isolated and combined rod and cone vision

(A–C) Results of Experiment 2.1 for rod vision (A), cone vision (B), and LMSR (C, combined rod and cone) visual conditions at the same mesopic light level using different contrast for the inducers to achieve maximum contrasts at each condition. We plotted normalized effect values for SBC versus WI induction. The normalized effect quantifies the strength of the induction for both stimuli. Effects equal to zero mean no induction. Gray, green and blue circles represent individual data, black circles represent the mean values, and solid black lines represent 95% confidence intervals. See also Figure S6.

induction than cone vision (Figure 5D, $t(10) = 3.76$, $p = 0.0037$), while rod and cone vision produced similar contrast induction (Figure 5E, $t(10) = 0.19$, $p = 0.85$). A control experiment confirmed that there was no bias in the absence of an inducing field (Figure 5F, ($t(10) = 0.21$, $p = 0.83$).

Due to the agreement between the results of the different experiments, we can conclude that rod and cone vision give rise to different brightness percepts but only for the assimilation induction. In general, brightness theories and models do not incorporate a differentiation between rod and cone vision,[8,44] therefore to propose an explanation of our results we need to test new hypotheses in a known conceptual framework.

Experiment 3. The role of transparency perception

Brightness induction can be a powerful tool to study interpretation of the scene. Since in our case the differences found in assimilation cannot be accounted for by low-level spatial summation (Experiment 1.2), we tested if a top-down mechanism can mediate our results. One possible explanation for our assimilation results is based on the scission theory.[45] Following this theory, the WI stimulus is decomposed into different layers, the gray patches in this display are perceived as transparent surfaces, therefore part of the brightness of these patches is attributed to the background. From studies 1 and 2, rod vision might trigger a different transparency perception than cone vision. For example, we can predict that the perceptual transparency triggered by the patches on the bright bars should be perceived as darker for rods than for cones.

We have tested how transparency is perceived at twilight conditions, where rods dominate vision. We found that three transparent samples (Opacity: 2%, 36%, and 71%, where opacity is computed as the reciprocal of transparency), seen under low mesopic conditions, were perceived more opaque (i.e., less transparent) than when they were seen under photopic conditions [$F(1, 16) = 31.65$, $p < 0.0001$], in particular for medium and low values of transparency (Sidak's test: $p < 0.0001$, $p = 0.0301$, respectively). This new finding about transparency perception in low light levels can explain the results of our previous experiments based on interpretation of the assimilation scene as transparent layers. Since stimuli are perceived as less transparent in twilight conditions than in daylight conditions (Figure 6), we can confirm the prediction from our main results in the framework of the scission theory.

DISCUSSION

The main result from this work is that brightness assimilation is increased in rod vision while brightness contrast is not altered in comparison to cone vision (Figures 5D and 5E). These results are similar to those found in an experiment when changing light adaptation from low mesopic to photopic light levels using a regular monitor (Figures 1B and 1C). Most importantly, we found that the increased assimilation effect could not be explained by low spatial resolution in rod vision, because it was also present in a stimulus with smoothed edges (Figure 1D). Transparency can pose challenging situations under rod vision.[46] Here, we show that the opacity of transparent media is overestimated in low light levels (Figure 6).

Our visual system uses information from the surroundings to interpret the properties of a central object. This concept applies to several visual attributes, among them, brightness perception. The assimilation stimulus that we used here is the White's illusion (WI).[1] This illusion has found explanations from a plethora of brightness theories (see below), Here, we show that the scission theory[45] can account for our assimilation results. We argue that inferences about the scene in assimilation displays can affect the appearance of a central patch.[7] This is especially true for rod vision, where challenging circumstances cause perceptual ambiguities that are solved by perceptual inferences.[17] In this context, and following the scission theory, the WI stimulus is affected by the different rod perception of transparent media that we found in experiment 3. Due to rod vision causing a darker transparency perception, the test patches on the bright bars of the WI stimulus are perceived darker for rods than for cones in studies 1 and 2.

However, why was this effect not found for brightness contrast? The contrast stimulus used here (SBC) is a very well-known effect studied since the 19th century[2,47] Recently, Sinha et al. have shown that this brightness induction is processed before binocular fusion, and it appears immediately after the

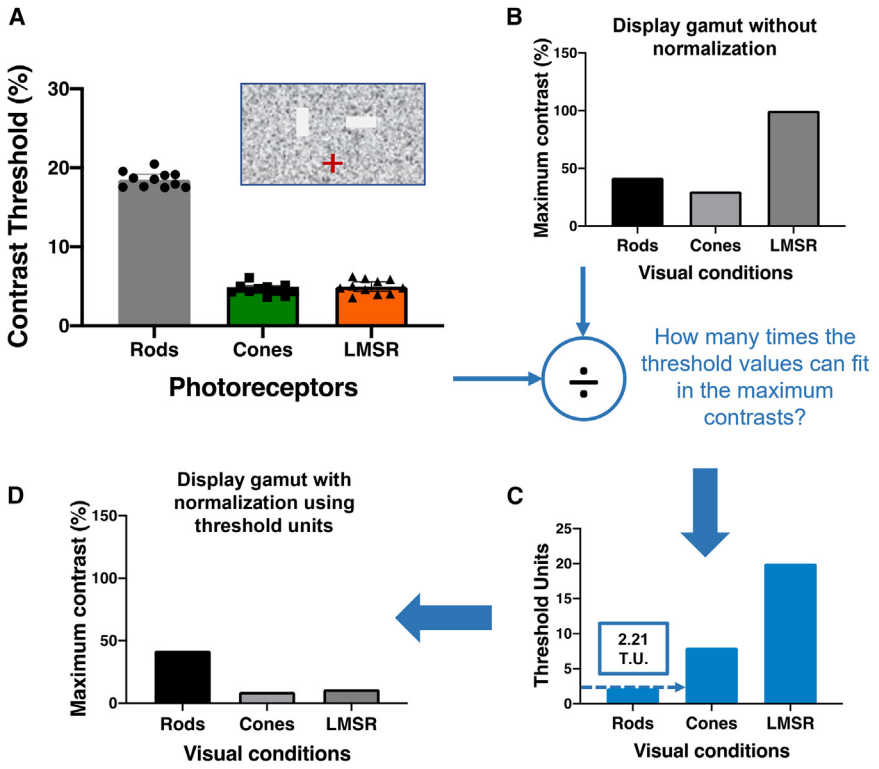

Figure 4. Normalization of the stimulus inducers considering differences in contrast thresholds between visual conditions

(A) Discrimination contrast thresholds of Experiment 2.2 for the three visual conditions: Rod vision, cone vision and combined cones and rods (LMSR). Bars represent the mean values, black data points correspond to individual data, error bars represent 95% confidence intervals. A representation of the stimulus used in this experiment is depicted in the inset (see text for more details). The normalization procedure is schematized in panels B – D.

(B) The Maximum contrasts available from the display after applying silent substitution.

(C) Number of threshold units for each visual condition that is possible to generate in the display.

(D) Normalized maximum contrast considering visual conditions matched at the same number of threshold units (2.21 T.U.).

sight-onset in children that were surgically treated for congenital cataract removal,[48] therefore these findings suggest that SBC effect is innate and processed early in the visual stream, ruling out high-level explanations.

Regarding the comparison of our results with previous studies, only one previous report has used a similar methodological approach to ours. Sun et al.,[37] using silent substitution, reported that rod modulation of a surrounding inducer can generate contrast brightness induction in a central patch at 10 deg. from the fovea, in agreement with our results (Figures 3A and 5A). They used a flickering nulling technique consisting in matching induced brightness in the center with a temporally modulated central light. If there is a complete match, the central stimulus should appear steady. They found that induced modulation at 1 Hz could be canceled with nulling modulation of rods and cones at mesopic levels lower than 1 phot. Td. However, for higher light levels the canceling modulation failed. Since Sun et al's results are based on flickering stimuli and we are concerned with simultaneous steady brightness matching, our findings cannot be interpreted in Sun et al's framework.

Lightness and brightness theories

In this study, we asked participants to judge the brightness of the stimuli. We discussed lightness and brightness judgments indistinctly, since brightness and lightness attributes can be considered equivalent under uniform illumination.[7,49,50]

The SBC and WI stimuli have received large attention in research and many theories and models have competed to explain them. Roughly, explanations of lightness/brightness induction have followed two main traditions. One explanation relies on high-order cognitive inferences about the visual environment, for example, the anchoring theory,[51] the scission theory,[52] etc. Another tradition explains induction based on low-level mechanisms, for example, spatial filtering.[53–55] However, the physiological basis of these low-level approaches starts in the visual cortex,[56] since there is evidence of the role of these areas in brightness perception.[57,58] To our knowledge, no lightness/brightness theory has considered seriously the role of different photoreceptors, even though several studies showed the importance of retinal light adaptation mechanisms in the perception of brightness.[59–62] Our study was not meant to generate evidence in favor of one or another approach but to study the role of rod versus cone vision. Furthermore, we showed that both traditions need to be considered to disentangle the complexity of brightness induction.

Early visual processing

From the point of view of visual processing, rods have separate pathways only at the retinal level. In humans, rod information does not reach an exclusive ganglion cell, but interacts with cone signals at the photoreceptor level (gap junctions) and at the cone bipolar cell level through rod bipolar/amacrine AII cells.[63–65] Therefore, a difference between rod vision and cone vision for the White's illusion means that retinal differences can trigger important perceptual effects and highlights the important role of early visual processing.

Conclusion

Under rod vision, brightness perception of complex stimuli is challenging. Our visual system adopts different strategies to solve the ambiguity posed by rod vision depending on whether the induction is assimilation or contrast. For brightness assimilation, interpretation of the scene seems to be solved by

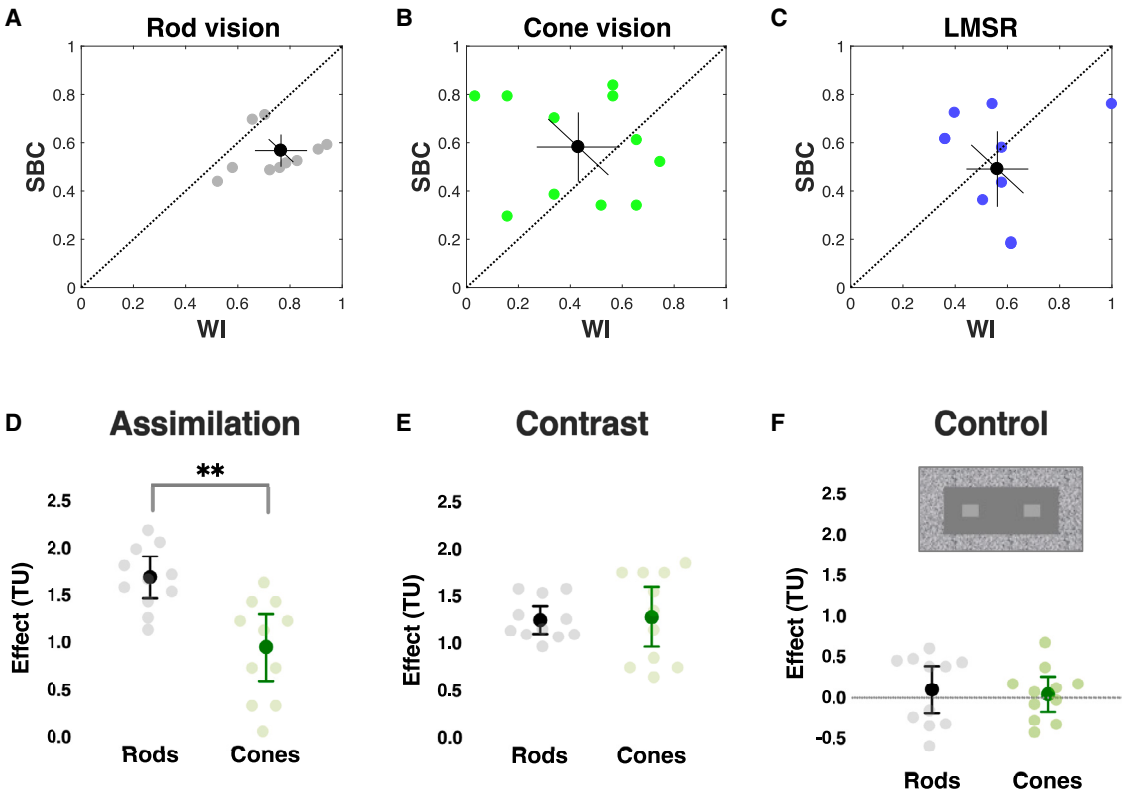

Figure 5. Brightness induction for isolated and combined rod and cone vision after normalization

(A–C) Results from Experiment 2.3 organized to compare WI and SBC for each visual condition: rod vision (A), cone vision (B) and LMSR (C). We plotted the normalized effect values for SBC versus WI induction; the normalization was with respect to the maximum possible TU (2.21). Effects equal to zero mean no induction. In panels A-B, colored (gray, green and blue) circles represent individual data, black circles represent the mean values, and solid black lines represent 95% confidence intervals.

(D–F) Results of Experiment 2.3. sorted out to compare brightness induction for rod and cone vision. For these panels the effect is shown in threshold units. For the assimilation stimuli (D), the induction effect is larger for rods than for cones. For the contrast stimuli (E), there was no significant difference between rod and cone vision. Small circles represent individual observers; large circles represent the average across observers. No effect was found for a control condition (F). A representation of the stimulus used for the control condition is shown in the inset. Error bars represent 95% confidence intervals in D–F. Differences between groups are indicated as (**) for $p < 0.01$. See also Figure S6.

high-order inferences. For brightness contrast, the differences between rod and cone vision do not lead to a different visual percept. This may be because this induction relies strongly on low-level mechanisms[48] and there is no need of a high-order inference to interpret the visual scene. Our study emphasizes the important role of the photoreceptors and the retinal circuits in the construction of the visual percept.

Limitations of the study

The LMSR condition consists of the same contrast excitation for rods and cones. Therefore, it might favor cone contributions since the LMSR stimuli were not weighted regarding threshold units, the weighted contributions were not tested, and it is outside the scope of the current study. Furthermore, different degrees of participation of cones and rods in the combined LMSR condition could provide a way to understand how rods and cones are combined to produce the brightness induction, as it was tested before for pupil control.[66] With our current experiments, we cannot talk about the nature of this combination. Cone information is conveyed by three main post-receptor pathways that correspond to the magno-, parvo-, and koniocellular layers of the lateral geniculate nucleus for visual processing,[67] producing different perceptual and detection effects.[31,68] Here, we only analyzed the combined excitatory contribution in the magnocellular pathway, which represents the combined excitation of three types of cones (L, M, and S) and rods. Also, the photopigment melanopsin in some conditions can contribute to brightness perception.[69–71] However, in our experimental conditions, its contribution should be negligible. This is because the mean background adapting light level (~20 phot. Td) in Experiment 2 and the low mesopic condition of Experiment 1 was below the melanopsin activation threshold,[72] as melanopsin activation in vision is only evident above 200 phot. Td[73] (Figure S4). In the photopic condition of Experiment 1, a potential contribution of melanopsin cannot be ruled out (Table S1); however, due to the short presentation time of the stimuli (0.5 s) and that the sluggish response of melanopsin in comparison to rods and cones, a potential

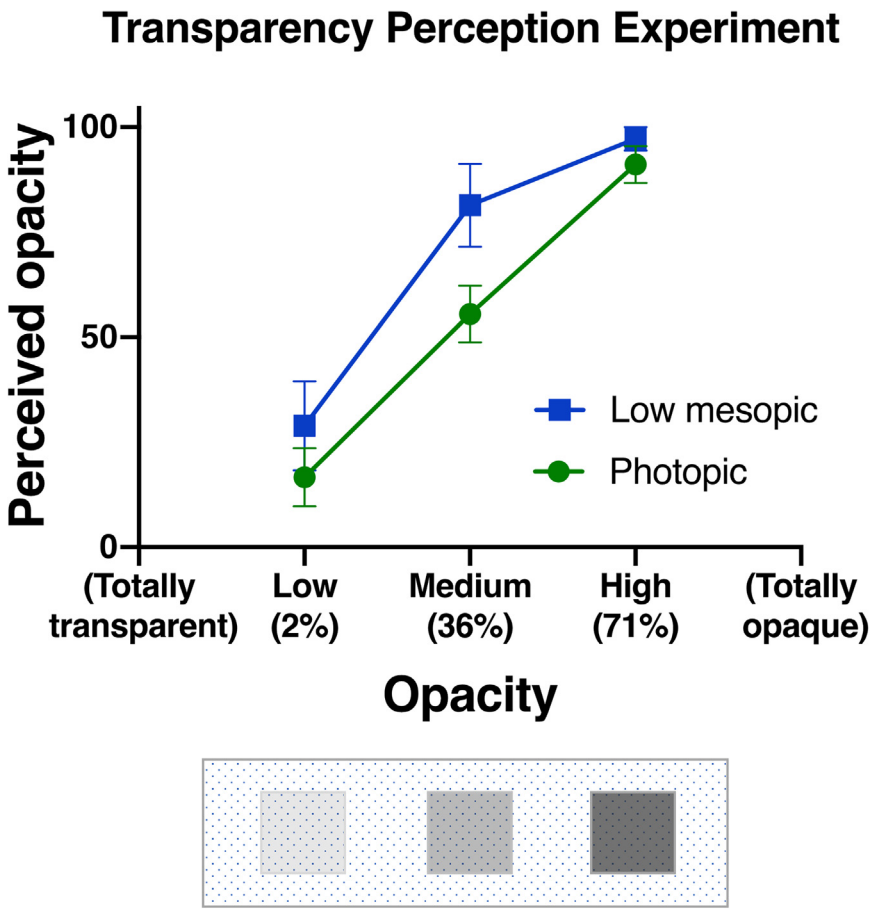

Figure 6. Transparency perception at different light levels

Results of Experiment 3 for the two light adaptation conditions tested: Low mesopic (blue) and Photopic (green). Observers freely scaled the perceived opacity of three samples (Low, Medium and High) from 0 to 100.

Schematic representation of the three transparent samples is shown below the data plot. Error bars represent 95% confidence interval.

contribution of melanopsin seems improbable. Finally, we tested two well-known types of brightness induction stimuli, the WI and the SBC; however, there is a vast amount of induction stimuli that could be considered.[74]

RESOURCE AVAILABILITY

Lead contact

Requests for further information and resources should be directed to and will be fulfilled by the lead contact, Dr. Pablo A. Barrionuevo (pbarrionuevo@herrera.unt.ed.ar).

Materials availability

This study did not generate new materials.

Data and code availability

- Psychophysical data have been deposited at Figshare and are publicly available as of the date of publication at https://doi.org/10.6084/m9.figshare.27312048.
- This paper does not report original code.
- Any additional information required to reanalyze the data reported in this paper is available from the lead contact upon request.

ACKNOWLEDGMENTS

This project has received funding from the German Research Foundation (DFG) - project number 222641018 - SFB/TRR 135 TP C2 and B2, the European Research Council (ERC) under the European Union's Horizon 2020 research and innovation program (grant agreement No 101001250, project "SENCES") to A.C.S., and the National Scientific and Technical Research Council (CONICET) – project code: PIBAA 1234 to P.A.B.

AUTHOR CONTRIBUTIONS

Conceptualization, P.A.B., A.C.S., and K.R.G.; Methodology, P.A.B.; Investigation, P.A.B.; Writing – Original Draft, P.A.B.; Writing – Review and Editing, P.A.B., A.C.S., and K.R.G; Funding Acquisition, P.A.B., A.C.S., and K.R.G.; Resources, A.C.S. and K.R.G.; Visualization, P.A.B.

DECLARATION OF INTERESTS

The authors declare no competing interests.

STAR★METHODS

Detailed methods are provided in the online version of this paper and include the following:

- KEY RESOURCES TABLE
- EXPERIMENTAL MODEL AND STUDY PARTICIPANT DETAILS
- METHOD DETAILS
  - Apparatus
  - Stimuli
  - Procedure
- QUANTIFICATION AND STATISTICAL ANALYSIS

SUPPLEMENTAL INFORMATION

Supplemental information can be found online at https://doi.org/10.1016/j.isci.2024.111609.

Received: July 4, 2024
Revised: October 7, 2024
Accepted: December 12, 2024
Published: January 4, 2025

REFERENCES

1. White, M. (1979). A new effect of pattern on perceived lightness. Perception *8*, 413–416. https://doi.org/10.1068/p080413.
2. Chevreul, M.E. (1855). The Principles of Harmony and Contrast of Colours, and Their Applications to the Arts (Brown, Green, and Longmans: Longman).
3. Cao, D., Lee, B.B., and Sun, H. (2010). Combination of rod and cone inputs in parasol ganglion cells of the magnocellular pathway. J. Vis. *10*, 4. https://doi.org/10.1167/10.11.4.
4. Aguilar, M., and Stiles, W.S. (1954). Saturation of the Rod Mechanism of the Retina at High Levels of Stimulation. Opt. Acta Int. J. Opt. *1*, 59–65. https://doi.org/10.1080/713818657.
5. Uprety, S., Adhikari, P., Feigl, B., and Zele, A.J. (2022). Melanopsin photoreception differentially modulates rod-mediated and cone-mediated human temporal vision. iScience *25*, 104529. https://doi.org/10.1016/j.isci.2022.104529.
6. Kingdom, F.A.A. (2011). Lightness, brightness and transparency: a quarter century of new ideas, captivating demonstrations and unrelenting controversy. Vis. Res. *51*, 652–673. https://doi.org/10.1016/j.visres.2010.09.012.
7. Gilchrist, A.L. (2006). Seeing Black and White (Oxford University Press).
8. Murray, R.F. (2021). Lightness Perception in Complex Scenes. Annu. Rev. Vis. Sci. *7*, 417–436. https://doi.org/10.1146/annurev-vision-093019-115159.
9. Zele, A.J., and Cao, D. (2014). Vision under mesopic and scotopic illumination. Front. Psychol. *5*, 1594. https://doi.org/10.3389/fpsyg.2014.01594.
10. Grimes, W.N., Songco-Aguas, A., and Rieke, F. (2018). Parallel Processing of Rod and Cone Signals: Retinal Function and Human Perception. Annu. Rev. Vis. Sci. *4*, 123–141. https://doi.org/10.1146/annurev-vision-091517-034055.
11. Stockman, A., and Sharpe, L.T. (2006). Into the twilight zone: the complexities of mesopic vision and luminous efficiency. Ophthalmic Physiol. Opt. *26*, 225–239. https://doi.org/10.1111/j.1475-1313.2006.00325.x.
12. Hess, R.F., Sharpe, L.T., and Nordby, K. (1990). Night Vision: Basic, Clinical and Applied Aspects (Cambridge University Press).
13. Gegenfurtner, K.R., Mayser, H., and Sharpe, L.T. (1999). Seeing movement in the dark. Nature *398*, 475–476. https://doi.org/10.1038/19004.
14. Ennis, R., Toscani, M., and Gegenfurtner, K.R. (2017). Seeing lightness in the dark. Curr. Biol. *27*, R586–R588. https://doi.org/10.1016/j.cub.2017.05.008.
15. Buck, S.L. (2001). What is the hue of rod vision? Color Res. Appl. *26*, S57–S59. https://doi.org/10.1002/1520-6378(2001)26:1+<::AID-COL13>3.0.CO;2-J.
16. Pokorny, J., Lutze, M., Cao, D., and Zele, A.J. (2006). The color of night: Surface color perception under dim illuminations. Vis. Neurosci. *23*, 525–530. https://doi.org/10.1017/S0952523806233492.
17. Gloriani, A.H., and Schütz, A.C. (2019). Humans Trust Central Vision More Than Peripheral Vision Even in the Dark. Curr. Biol. *29*, 1206–1210. https://doi.org/10.1016/j.cub.2019.02.023.
18. Schneeweis, D.M., and Schnapf, J.L. (1995). Photovoltage of rods and cones in the macaque retina. Science *268*, 1053–1056. https://doi.org/10.1126/science.7754386.
19. Barlow, R.B. (1980). Brightness sensation and pupil reflex in normals, rod monochromats, and patients with retinitis pigmentosa. Adv. Ophthalmol. *41*, 175–177.
20. Zele, A.J., Dey, A., Adhikari, P., and Feigl, B. (2020). Rhodopsin and melanopsin contributions to human brightness estimation. JOSA A *37*, A145–A153. https://doi.org/10.1364/JOSAA.379182.
21. Chen, B., MacLeod, D.I., and Stockman, A. (1987). Improvement in human vision under bright light: grain or gain? J. Physiol. *394*, 41–66. https://doi.org/10.1113/jphysiol.1987.sp016859.
22. Sharpe, L.T., Whittle, P., and Nordby, K. (1993). Spatial integration and sensitivity changes in the human rod visual system. J. Physiol. *461*, 235–246. https://doi.org/10.1113/jphysiol.1993.sp019511.
23. Barlow, H.B. (1958). Temporal and spatial summation in human vision at different background intensities. J. Physiol. *141*, 337–350.
24. Drum, B. (1981). Rod—cone interaction in the dark-adapted fovea. JOSA *71*, 71–74.
25. Buck, S.L., and Brandt, J.L. (1995). The range of simultaneous scotopic contrast colors. In Colour Vision Deficiencies XII: Proceedings of the twelfth Symposium of the International Research Group on Colour Vision Deficiencies, held in Tübingen, Germany July 18–22, 1993, B. Drum, A.J. Adams, C.R. Cavonius, S.J. Dain, G. Haegerstrom-Portnoy, K. Kitahara, K. Knoblauch, A. Kurtenbach, B.B. Lee, and J. Mollon, eds. (Springer Netherlands), pp. 309–316. https://doi.org/10.1007/978-94-011-0507-1_36.
26. Stabell, U., and Stabell, B. (1975). The effect of rod activity on colour matching functions. Vis. Res. *15*, 1119–1123. https://doi.org/10.1016/0042-6989(75)90010-3.
27. Hollins, M. (1971). Brightness contrast at low luminances. Vis. Res. *11*, 1459–1472. https://doi.org/10.1016/0042-6989(71)90066-6.
28. McCann, J. (2012). Color assimilation and contrast near absolute threshold. In Color Imaging XVII: Displaying, Processing, Hardcopy, and Applications (SPIE), pp. 15–23. https://doi.org/10.1117/12.912003.
29. McCourt, M.E. (1990). Disappearance of grating induction at scotopic luminances. Vis. Res. *30*, 431–437. https://doi.org/10.1016/0042-6989(90)90084-X.
30. Hexley, A.C., Yöntem, A.Ö., Spitschan, M., Smithson, H.E., and Mantiuk, R. (2020). Demonstrating a multi-primary high dynamic range display system for vision experiments. JOSA A *37*, A271–A284. https://doi.org/10.1364/JOSAA.384022.
31. Cormenzana Méndez, I., Martín, A., O'Donell, B., Cao, D., and Barrionuevo, P.A. (2022). Temporal integration of rod signals in luminance and chromatic pathways. JOSA A *39*, 1782–1793. https://doi.org/10.1364/JOSAA.462581.
32. Bayer, F.S., Paulun, V.C., Weiss, D., and Gegenfurtner, K.R. (2015). A tetrachromatic display for the spatiotemporal control of rod and cone stimulation. J. Vis. *15*, 15. https://doi.org/10.1167/15.11.15.
33. Nugent, T.W., and Zele, A.J. (2022). A five-primary Maxwellian-view display for independent control of melanopsin, rhodopsin, and three-cone opsins on a fine spatial scale. J. Vis. *22*, 20. https://doi.org/10.1167/jov.22.12.20.
34. Allen, A.E., Martial, F.P., and Lucas, R.J. (2019). Form vision from melanopsin in humans. Nat. Commun. *10*, 2274. https://doi.org/10.1038/s41467-019-10113-3.
35. Barrionuevo, P.A., Preciado, O.U., Sandoval Salinas, M.L., and Issolio, L.A. (2022). Optical stimulation systems for studying human vision. In Progress in Brain Research Circadian and Visual Neuroscience, N. Santhi and M. Spitschan, eds. (Elsevier), pp. 13–32.
36. Nugent, T.W., Carter, D.D., Uprety, S., Adhikari, P., Feigl, B., and Zele, A.J. (2023). Protocol for isolation of melanopsin and rhodopsin in the human eye using silent substitution. STAR Protoc. *4*, 102126. https://doi.org/10.1016/j.xpro.2023.102126.

37. Sun, H., Pokorny, J., and Smith, V.C. (2001). Brightness induction from rods. J. Vis. *1*, 32–41. https://doi.org/10.1167/1.1.4.

38. Mach, E. (1865). Über die Wirkung der räumlichen Vertheilung des Lichtreizes auf die Netzhaut: vorgelegt in der Sitzung am 3. October 1865 (K. k. Hof- und Staatsdruckerei).

39. Hess, R.F., and Nordby, K. (1986). Spatial and temporal limits of vision in the achromat. J. Physiol. *371*, 365–385. https://doi.org/10.1113/jphysiol.1986.sp015981.

40. Krauskopf, J., Zaidi, Q., and Mandler, M.B. (1986). Mechanisms of simultaneous color induction. J. Opt. Soc. Am. *3*, 1752–1757. https://doi.org/10.1364/JOSAA.3.001752.

41. Wagner, I., and Schütz, A.C. (2023). Interaction of dynamic error signals in saccade adaptation. J. Neurophysiol. *129*, 717–732. https://doi.org/10.1152/jn.00419.2022.

42. MacAdam, D.L. (1942). Visual Sensitivities to Color Differences in Daylight. J. Opt. Soc. Am. *32*, 247. https://doi.org/10.1364/JOSA.32.000247.

43. Cao, D., Pokorny, J., and Smith, V.C. (2005). Matching rod percepts with cone stimuli. Vis. Res. *45*, 2119–2128.

44. Anderson, B.L. (2003). Perceptual organization and White's illusion. Perception *32*, 269–284.

45. Anderson, B.L. (1997). A Theory of Illusory Lightness and Transparency in Monocular and Binocular Images: The Role of Contour Junctions. Perception *26*, 419–453. https://doi.org/10.1068/p260419.

46. Nordby, K. (1990). Vision in a Complete Achromat: A Personal Account. In Night Vision: Basic, Clinical and Applied Aspects, R.F. Hess, L.T. Sharpe, and K. Nordby, eds. (Cambridge University Press).

47. Viénot, F. (2002). Michel-Eugène Chevreul: From laws and principles to the production of colour plates. Color Res. Appl. *27*, 4–14. https://doi.org/10.1002/col.10000.

48. Sinha, P., Crucilla, S., Gandhi, T., Rose, D., Singh, A., Ganesh, S., Mathur, U., and Bex, P. (2020). Mechanisms underlying simultaneous brightness contrast: Early and innate. Vis. Res. *173*, 41–49. https://doi.org/10.1016/j.visres.2020.04.012.

49. Radonjić, A., Pearce, B., Aston, S., Krieger, A., Dubin, H., Cottaris, N.P., Brainard, D.H., and Hurlbert, A.C. (2016). Illumination discrimination in real and simulated scenes. J. Vis. *16*, 2. https://doi.org/10.1167/16.11.2.

50. Blakeslee, B., Reetz, D., and McCourt, M.E. (2008). Coming to terms with lightness and brightness: effects of stimulus configuration and instructions on brightness and lightness judgments. J. Vis. *8*, 1–14. https://doi.org/10.1167/8.11.3.

51. Gilchrist, A., Kossyfidis, C., Bonato, F., Agostini, T., Cataliotti, J., Li, X., Spehar, B., Annan, V., and Economou, E. (1999). An anchoring theory of lightness perception. Psychol. Rev. *106*, 795–834.

52. Anderson, B.L. (1997). A theory of illusory lightness and transparency in monocular and binocular images: the role of contour junctions. Perception *26*, 419–453.

53. Blakeslee, B., and McCourt, M.E. (2004). A unified theory of brightness contrast and assimilation incorporating oriented multiscale spatial filtering and contrast normalization. Vis. Res. *44*, 2483–2503. https://doi.org/10.1016/j.visres.2004.05.015.

54. Kingdom, F.A., McCourt, M.E., and Blakeslee, B. (1997). In defence of "lateral inhibition" as the underlying cause of induced brightness phenomena: a reply to Spehar, Gilchrist and Arend. Vis. Res. *37*, 1039–1047.

55. Morrone, M.C., and Burr, D.C. (1988). Feature detection in human vision: a phase-dependent energy model. Proc. R. Soc. Lond. B Biol. Sci. *235*, 221–245. https://doi.org/10.1098/rspb.1988.0073.

56. Kingdom, F.A.A. (2011). Lightness, brightness and transparency: A quarter century of new ideas, captivating demonstrations and unrelenting controversy. Vis. Res. *51*, 652–673. https://doi.org/10.1016/j.visres.2010.09.012.

57. Rossi, A.F., Rittenhouse, C.D., and Paradiso, M.A. (1996). The representation of brightness in primary visual cortex. Science *273*, 1104–1107.

58. Perna, A., Tosetti, M., Montanaro, D., and Morrone, M.C. (2005). Neuronal Mechanisms for Illusory Brightness Perception in Humans. Neuron *47*, 645–651. https://doi.org/10.1016/j.neuron.2005.07.012.

59. Shapley, R., and Enroth-Cugell, C. (1984). Visual adaptation and retinal gain controls. Prog. Retin. Res. *3*, 263–346.

60. Shevell, S.K., Holliday, I., and Whittle, P. (1992). Two separate neural mechanisms of brightness induction. Vis. Res. *32*, 2331–2340. https://doi.org/10.1016/0042-6989(92)90096-2.

61. Radonjić, A., Allred, S.R., Gilchrist, A.L., and Brainard, D.H. (2011). The Dynamic Range of Human Lightness Perception. Curr. Biol. *21*, 1931–1936. https://doi.org/10.1016/j.cub.2011.10.013.

62. Barrionuevo, P.A., Colombo, E.M., and Issolio, L.A. (2013). Retinal mesopic adaptation model for brightness perception under transient glare. J. Opt. Soc. Am. *30*, 1236–1247. https://doi.org/10.1364/JOSAA.30.001236.

63. Buck, S.L. (2004). Rod-cone interactions in human vision. In The visual neurosciences, pp. 863–878.

64. Sharpe, L.T., and Stockman, A. (1999). Rod pathways: the importance of seeing nothing. Trends Neurosci. *22*, 497–504.

65. Sterling, P. (2004). How Retinal Circuits Optimize the Transfer of Visual Information. In The Visual Neurosciences, L. Chalupa and J. Warner, eds. (MIT Press), pp. 234–259.

66. Barrionuevo, P.A., Nicandro, N., McAnany, J.J., Zele, A.J., Gamlin, P., and Cao, D. (2014). Assessing Rod, Cone, and Melanopsin Contributions to Human Pupil Flicker Responses. Invest. Ophthalmol. Vis. Sci. *55*, 719–727. https://doi.org/10.1167/iovs.13-13252.

67. Lee, B.B. (2011). Visual pathways and psychophysical channels in the primate. J. Physiol. *589*, 41–47. https://doi.org/10.1113/jphysiol.2010.192658.

68. Cao, D., Pokorny, J., Smith, V.C., and Zele, A.J. (2008). Rod contributions to color perception: Linear with rod contrast. Vis. Res. *48*, 2586–2592. https://doi.org/10.1016/j.visres.2008.05.001.

69. Barrionuevo, P.A., Sandoval Salinas, M.L., and Fanchini, J.M. (2024). Are ipRGCs involved in human color vision? Hints from physiology, psychophysics, and natural image statistics. Vis. Res. *217*, 108378. https://doi.org/10.1016/j.visres.2024.108378.

70. Brown, T.M., Tsujimura, S.I., Allen, A.E., Wynne, J., Bedford, R., Vickery, G., Vugler, A., and Lucas, R.J. (2012). Melanopsin-Based Brightness Discrimination in Mice and Humans. Curr. Biol. *22*, 1134–1141. https://doi.org/10.1016/j.cub.2012.04.039.

71. Zele, A.J., Adhikari, P., Feigl, B., and Cao, D. (2018). Cone and melanopsin contributions to human brightness estimation. JOSA A *35*, B19–B25. https://doi.org/10.1364/JOSAA.35.000B19.

72. Zele, A.J., Adhikari, P., Cao, D., and Feigl, B. (2019). Melanopsin driven enhancement of cone-mediated visual processing. Vis. Res. *160*, 72–81. https://doi.org/10.1016/j.visres.2019.04.009.

73. Zele, A.J., Feigl, B., Adhikari, P., Maynard, M.L., and Cao, D. (2018). Melanopsin photoreception contributes to human visual detection, temporal and colour processing. Sci. Rep. *8*, 3842. https://doi.org/10.1038/s41598-018-22197-w.

74. Adelson, E.H. (2000). Lightness Perception and Lightness Illusions. In The new cognitive neurosciences, M. Gazzaniga, ed. (MIT Press), pp. 339–351.

75. Kleiner, M., Brainard, D., and Pelli, D. (2007). What's new in Psychtoolbox-3? Perception *36*, 1.

76. Brainard, D.H. (1997). The Psychophysics Toolbox. Spatial Vis. *10*, 433–436.

77. Pelli, D.G. (1997). The VideoToolbox software for visual psychophysics: transforming numbers into movies. Spat. Vista *10*, 437–442.

78. Cornelissen, F.W., Peters, E.M., and Palmer, J. (2002). The Eyelink Toolbox: Eye tracking with MATLAB and the Psychophysics Toolbox. Behav. Res. Methods Instrum. Comput. *34*, 613–617. https://doi.org/10.3758/BF03195489.

79. Heinemann, E.G. (1955). Simultaneous brightness induction as a function of inducing- and test-field luminances. J. Exp. Psychol. *50*, 89–96. https://doi.org/10.1037/h0040919.

80. Estévez, O., and Spekreijse, H. (1982). The "silent substitution" method in visual research. Vis. Res. *22*, 681–691.

81. Smith, V.C., and Pokorny, J. (1975). Spectral sensitivity of the foveal cone photopigments between 400 and 500 nm. Vis. Res. *15*, 161–171. https://doi.org/10.1016/0042-6989(75)90203-5.

82. CIE (1951). Commission Internationale de l'Eclariage Proceedings, 1951 (Bureau Central de la CIE).

83. Pokorny, J., and Cao, D. (2010). Rod and cone contributions to mesopic vision. In CIE Symposium "Lighting Quality & Energy Efficiency, *x035*, pp. 9–20.

84. Preciado, O.U., Sandoval Salinas, M.L., Issolio, L.A., and Barrionuevo, P.A. (2023). Systems for selective stimulation of retinal pathways. Opt. Pura Apl. *56*, 51150. https://doi.org/10.7149/OPA.56.2.51150.

85. Watson, A.B., and Pelli, D.G. (1983). Quest: A Bayesian adaptive psychometric method. Percept. Psychophys. *33*, 113–120. https://doi.org/10.3758/BF03202828.

86. Barrionuevo, P.A., Schütz, A.C., and Gegenfurtner, K.R.. Dataset from the study "Increased brightness assimilation in rod vision". 2020 Dataset Figshare. https://doi.org/10.6084/m9.figshare.27312048.

STAR★METHODS

KEY RESOURCES TABLE

REAGENT or RESOURCE	SOURCE	IDENTIFIER
Deposited data		
Psychophysical data	This study	Database: https://doi.org/10.6084/m9.figshare.27312048
Software and algorithms		
MATLAB	The MathWorks	https://www.mathworks.com/products/matlab.html
Psychtoolbox	Psychtoolbox	http://psychtoolbox.org/
Prism	GraphPad Software	https://www.graphpad.com/features
Other		
Eyelink 1000+ eye tracker	SR Research	https://www.sr-research.com/products/eyelink-1000-plus/
Tetra-chromatic PROPixx projector	VPixx Technologies	https://vpixx.com/products/propixx-multispectral/
Spectroradiometer SpectroCAL	Cambridge Research Systems	https://www.crsltd.com/tools-for-vision-science/light-measurement-display-calibation/spectrocal-mkii-spectroradiometer/
Spectroradiometer CS-3000	Konica Minolta	https://sensing.konicaminolta.us/us/products/cs-3000-spectroradiometer/
Optical Filters	LEE Filters	https://leefilters.com/

EXPERIMENTAL MODEL AND STUDY PARTICIPANT DETAILS

In total, sixteen observers participated in this study and completed at least one experiment (nine females, age mean ± s.d.: 34.25 ± 6.5 y.o.). Twelve of them participated in more than one experiment. Four observers completed Experiment 1.1 (three females, age mean ± s.d.: 34 ± 6.6 y.o.). Seven observers completed Experiment 1.2 (five females, age mean ± s.d.: 35.7 ± 7.1 y.o.). Ten observers completed Experiment 2.1 (six females, age mean ± s.d.: 33.2 ± 5.8 y.o.). Ten observers completed Experiment 2.2 (five females, age mean ± s.d.: 33.3 ± 6.2 y.o.). Eleven observers completed Experiment 2.3 (six females, age mean ± s.d.: 34.18 ± 6.6 y.o.). Nine observers completed Experiment 3 (six females, age mean ± s.d.: 34.18 ± 6.6 y.o.). All the participants in this study had normal or corrected to normal visual acuity, and normal color vision. The participants provided informed consent, were recruited in the cities of Marburg and Giessen, Germany with middle socioeconomic status. They have different ethnical backgrounds but most of them have European origin (nine observers). The experimental procedure followed the tenants of the Declaration of Helsinki and was approved by the local ethics committee of the Psychology Department at Marburg University (proposal number 2021-71k). All participants gave informed consent to participate in this study.

METHOD DETAILS

Apparatus

Experiment 1: The visual stimuli were generated with the software Psychtoolbox 3[75–77] in the computing environment Matlab (MathWorks, Natick, MA, USA). An LCD monitor (VPixx Technologies, Saint-Bruno, QC Canada) was used to show the stimuli. Neutral density filters (LEE Filters, Burbank, CA, USA) were used to cover entirely the screen of the monitor. These filters were placed between layers of polymethyl methacrylate (PMMA) and mounted in a black metal frame positioned in front of the monitor. The observer used a chin rest to stabilize the head and see the monitor, which was located at 61.5 cm from their eyes. The monitor measured 52 cm (Vertical) × 29 cm (Horizontal), provided a spatial resolution of 43 (V) x 48 (H) pixels per degree, and its luminance range was linearized. The room was totally darkened during experimentation.

Experiment 2: To generate the stimuli, we used an ad-hoc tetra-chromatic projector (VPixx Technologies, Saint-Bruno, QC, Canada). In this projector, besides the traditional red, green, and blue primaries, a fourth yellow primary was implemented (Figure 1A). The image was projected into a rear projection screen (Stewart Filmscreen, Torrance, CA, USA). Using an eye-tracker (Eyelink 1000+, SR Research Ltd. Ontario, Canada) and the Eyelink toolbox,[78] we monitored the gaze position and pupil diameter of the observer. To obtain a larger photoreceptor gamut, the image of the projector was filtered with two overlapped layers (Figure 2C) of a yellowish filter (765, LEE Filters, Burbank, CA, USA). The primaries' peak wavelength after filtering were: 618 nm (red), 529 nm (green), 461 nm (blue), and 582 nm (yellow). The luminance output of the projector was linearized. The visible projection area measured 92 cm (V) × 52 cm (H), provided a spatial resolution of 39 (V) x 60 (H) pixels per degree. The room was totally darkened during

experimentation. The visual stimuli were generated with the software Psychtoolbox 3[75–77] in the computing environment Matlab (MathWorks, Natick, MA, USA) and verified using a spectroradiometer SpectroCAL (Cambridge Research Systems, Rochester, UK) (Figure S3). The participants were located 100 cm from the screen. Calibration of this system is explained in detail in the supplemental information (Figure S3. Calibration to apply silent substitution).

Experiment 3: We used three samples of 5 cm x 5 cm of neutral density filters (LEE Filters, Burbank, CA, USA). The opacities of the samples were 2%, 36%, and 71%, the opacities were computed as the inverse of the transmittance measured using a spectroradiometer (CS-3000, Konica Minolta, Japan). A white piece of paper with a pattern of points was used as a background (Figure 6). The room was totally darkened during experimentation and the samples were only illuminated indirectly by the screen described in Experiment 2 at a mesopic light level.

Stimuli

Inducing configurations consisted of 1) Assimilation (WI) condition: four gray patches (two reference and two test) embedded in four horizontal interleaved bright and dark inducing bars to form the White's illusion (Figure 1A)[1]; 2) Contrast (SBC) condition: two gray patches (reference and test) embedded in two bright and dark rectangles to shape the classical Simultaneous Brightness Contrast illusion (Figure 1A)[79]; and 3) Control condition: two gray patches (reference and test) embedded in a uniform dark rectangle (Figure 5F, inset). In this section light levels are expressed in photopic 2° cd/m^2, values at different units can be found in Tables S1 and S2.

Experiment 1

The stimuli were generated in the achromatic domain at two mean light levels (Photopic: 55.3 cd/m^2; and Low mesopic: 0.014 cd/m^2). Inducing bright and dark bars in the WI stimulus and the inducing bright (dark) rectangle in the SBC stimulus were set to the maximum and minimum luminance allowed by the monitor, respectively. Reference and test patches were initially set at the mean light levels, which was at 50% of the maximum luminance. The rectangular stimulus was located at 6° from the fixation cross. The stimulus subtended 4.65° (V) x 14.4° (H). Each embedded patch subtended 1.16°(V) x 1.49°(H). The fixation cross was surrounded by an oval ring to make it visible in low light levels. The oval subtended 0.84°(V) x 1.21°(H). The screen size in subtended degrees was 40.2° (V) x 25.3° (H). The fixation cross was at the center of the screen while the stimulus switched consecutively between up and down position with respect to the fixation cross to avoid afterimages as confounding factor. Further details about this experiment can be found in the supplemental information (Figures S1, S2, and S5).

Experiment 2

In this experiment package we employed the technique of silent substitution, which allows isolation of the responses of each photoreceptor type while silencing others in a non-invasive manner.[80] The method relies on the principle of univariance, where changes in wavelength components of the incident radiation cannot be distinguished from changes in the intensity of the incident radiation in the responses of photoreceptors.[35] Photoreceptor excitations (L, M, S, R) were computed based on the Smith and Pokorny cone fundamentals for the CIE 1964 10° Standard Observer.[81] Rod excitation (R) was computed based on the scotopic luminosity function.[82] The photoreceptor sensitivities were normalized based on matching the areas of the S and R sensitivities to the photopic sensitivity function [V(λ)] for a 1cd/m^2 equal energy spectrum, and 0.667 L + 0.33 M = 1 cd/m^2 [31]. To avoid apparition of chromatic aberrations in the image, all stimuli edges using the tetra-chromatic display were slightly smoothed. This procedure was conducted using an ad-hoc 2-D cumulative gaussian function applied to stimulus surfaces borders.

Silent substitution calculations were performed following the procedure outlined elsewhere.[36,83,84] In a nutshell, we generated a matrix with the excitations for each photoreceptor at the maximum intensity of the primary light sources. When this matrix is multiplied by a vector containing values between 0 and 1, we can generate different values of excitations. In other words, by dimerizing the primaries we could control the photoreceptor excitations. We used the inverse process to compute the dimerizing values that generate an excitation change in only one photoreceptor type (for example rods) while keeping the others constant (for example L, M, and S cones). The maximum possible change is limited by the gamut of the system, therefore in practical terms, we used an iterative procedure to find the best combinations of excitations to maximize the contrast gamut. Intended photoreceptor excitations were verified from spectral measurements of the stimuli. All stimuli had a baseline with the same 10° chromaticity (x = 0.52, y = 0.44) and a luminance of 1.92 phot. cd/m^2 (28 photopic Td). The screen subtended 27.5° (V) x 42.6° (H).

One of the advantages of silent substitution is that the same level of adaptation is used for isolated rod vision and isolated cone vision. In our case, the silent-substitution experiments were performed at one mesopic light level. For the range of Weber rod contrast used in this work (0 – 42%), cone stimulation was meant to remain constant. The silent substitution method allows for selective stimulation of one type of photoreceptor, however, during the generation of this stimulation certain assumptions are made that are not completely achieved by a real stimulation system even after calibration of the system, and the tabulated spectral sensitivities may vary for individual participants. Therefore, to avoid artifacts due to unwanted stimulation, we have followed two procedures: 1) Spectral verification: As certain assumptions about linearity, independence, additivity and spatial alignment considered for the computation might not be completely achieved in real setups, the final stimulus might have variations from the computed one. This procedure is included to assess the residual excitation in unwanted photoreceptors. A spectral verification procedure showed that residual cone excitation contrast was 2.7% (S), -0.9% (M) and -1% (L) when the rod increment was 41.5% (see Figure S4). These cone values are below the lowest cone contrast threshold (~4% see Figure 4). Melanopsin excitation contrast was 55.3% for the maximum rod excitation contrast, which is not surprising due to the high correlation of rhodopsin and melanopsin contrasts.[33] However, the overall light level was below melanopsin threshold as described in the supplemental information (Figure S4). 2) Individual calibration: Due to

individual variations in intraocular media and photopigment polymorphisms, the spectral sensitivity needs to be individually corrected. Although these variations might not be so important due to the limited age range and the healthy eye condition of our participants, to ensure correct stimulation and account for individual variations we used a brightness/color matching procedure. This procedure consisted in changing the primaries' intensities of a foveated rod-stimulating patch. Since there are no rods in the fovea this stimulus should not be discriminable from the background. If participants could discriminate the shape of the rod stimulus, they could adjust the intensities of two primaries until the stimulus disappeared or its shape could not be distinguished. Further characterization data of the stimulation system is shown in Figure S3.

Experiment 2.1: The inducing bright (dark) bars in the WI stimulus and the inducing bright (dark) rectangle in the SBC were set to the maximum contrasts (Rod vision: 36%, Cone vision: 26%; LMSR: 100%). The image of the inducing stimulus (in SBC, WI, and Control conditions) subtended 7.7° (V) and 18.3° (H) and was presented at 6.8° of a foveated fixation cross. To avoid the intrusion of afterimages, the fixation cross was presented alternately above or below the inducing stimulus in subsequent trials.

Experiment 2.2: The stimuli were composed of one vertical bar and one horizontal bar, they were presented extra-foveally above the fixation cross (Figure 4A).

Experiment 2.3: To compute the Threshold Units (TU), i.e., how many times the threshold contrast can be multiplied to reach the maximum contrast available due to gamut limitations, we divided the maximum contrast available for each visual condition (Rods = 42%, Cones = 30%, and LMSR = 100%) by the mean contrast threshold obtained (Figure 4). The lower maximum threshold units needed to achieve the maximum contrast was for rods (2.21 TU), therefore we normalized the maximum available contrast to reach 2.21 TU for each visual condition. Then, inducers were set to Michelson contrasts of ± 42% (Rod vision), ± 8.84% (Cone vision), and ± 11.05% (LMSR). Reference and test patches were initially set at 0 TU. The image of the inducing stimulus (in SBC, WI, and Control conditions) subtended 7.7° (V) and 18.3° (H) and was presented at 6.8° of a foveated fixation cross. To avoid the intrusion of afterimages, the fixation cross was presented alternately above or below the inducing stimulus in subsequent trials. An analysis of how the normalization by threshold units impacted in the results is included in the supplemental information (Figure S6. Effect of the normalization by threshold units).

Procedure

Experiment 1

Each session started with 2 min. of adaptation to the background light level. Then, a series of trials were presented. After each trial the participant had to answer the location (left or right) of the brighter patch. Before each session, participants were instructed about which parts of the visual stimulus (patches) they had to judge in terms of brightness and where they had to fixate. The stimulus was presented extrafoveally and during 0.5 s. The minimum inter-stimulus interval was of 2 s. With a limits method we determined five comparison luminance values. Then, through a constant stimuli paradigm, we obtained the point of subjective equality (PSE) between the brightness of the reference and test patches. We presented 20 trials for each comparison value, totaling 100 trials per condition. We computed the percentual effect (Weber contrast between the PSE and the reference luminance) for each condition. The task was binocular. A period of 20 min. of dark adaptation preceded the low mesopic condition.

Experiment 2

Before experimental sessions, every participant conducted a brightness-color matching calibration procedure to customize photoreceptor sensitivities and avoid artifacts due to residual unwanted excitations.[69] In each session participants dark-adapted for 15 minutes, then they light-adapt for 2 minutes to the background light level, after that, a succession of trials for a determined experimental condition appeared. The stimulus presentation in each trial was 1.5 s. An interstimulus interval (ISI) lasted 2 seconds or until the participant pressed the response button, the background light level with a spatial white noise (to reduce aftereffects) was maintained during the ISI.

Experiments 2.1 and 2.3: In each trial, the participants had to judge the brightness of two patches embedded in the inducing stimuli and select the brighter one. One of the patches had a reference excitation, while the other (test) patch changed the excitation trial by trial. Reference and test positions were randomly interchanged between left and right positions; therefore, the observers did not know beforehand their relative position. In each session, the participants conducted nine experimental conditions [three photoreceptor stimuli (Rods, Cones, and LMSR) by three inducing configurations (WI, SBC, and Control)]. The participants looked at the stimulus monocularly with their dominant eye. Through a gaze-contingent paradigm,[41] we ensured that the participants could perceive the stimulus foveally. Using this paradigm, the stimulus disappeared every time the participants moved their gaze more than 2.9 deg away from the fixation cross, therefore controlling that the study was conducted at the required eccentricity. Since the fixation cross was presented alternately above or below the inducing stimulus in subsequent trials, participants were asked to follow the fixation cross while the eye-position was controlled using the gaze-contingent paradigm.

Experiment 2.1: A Quest procedure[85] was used to obtain the matching value between the brightness of the test and the reference patch. The effect was computed as the Weber contrast between the final excitation of the test and the reference excitation, we normalized the results considering the maximum contrast for each condition (Figure 3). Ten participants performed this experiment.

Experiment 2.2: The stimuli were presented extra-foveally (Figure 5F), and the participants had to answer where the vertical bar (left or right) was located using a QUEST procedure[85] in a two-alternative-forced choice experiment.

Experiment 2.3: Following a staircase procedure, the inducing effect was computed as the difference (in terms of TU) between a reference patch (with a constant excitation) and the test patch excitation needed to match them in brightness. The subjective brightness matching was computed as the average of the last four presentations. Eleven participants performed this experiment.

Experiment 3: Observers freely estimated the opacity of the samples. They were instructed to rank how opaque the samples were between 0% (totally transparent) and 100% (totally opaque). We chose to rate the samples in terms of opacity (and not transparency) because this concept was more intuitive for the participants to rank. Specifically, the participants were instructed to ''rate how opaque the samples are''. To ensure that they were rating the intrinsic material property and the amount light passing through, they were also instructed to act as an instrument to measure the percentage of light that is blocked by the sheet. They had to provide a unique opacity value disregarding the environmental conditions. The transparent samples were shown one by one to the participants in a random order.

QUANTIFICATION AND STATISTICAL ANALYSIS

Statistical analyses of our data[86] were performed using the Matlab (Mathworks Inc.) and Prism (GraphPad Software LLC) software. The analyses performed can be found in the caption of Figure 1A and in the subsections of the results section: Experiment 1.1. Testing the effect of illumination level, Experiment 1.2. Testing the "poor resolution at low light levels" hypothesis, Experiment 2.1. Maximum stimulus contrasts, Experiment 2.3. Normalization by threshold units, and Experiment 3. The role of transparency perception. We performed paired t-tests (Experiments 2.1 and 2.3), two-way ANOVA (Experiments 1.1 and 3), and Sidak's (Experiments 1.1 and 3) and Tukey's (Experiment 1.2) post-hoc tests. The significance level was set at 5% in all analyses. Reported results include means and 95% confidence intervals in Figures 1, 3, 4, 5, and 6. Medians are shown in Figure 1. Single data points are reported in Figures 1, 3, and 5. Differences between groups are indicated as (**) for $p < 0.01$ (Figure 5D). In the results section, we also reported means with standard deviations (Experiments 2.1 and 2.3), and means (Experiment 2). In experiment 1, the contrast of the inducers was set to 100% for all conditions, therefore the effect was quantified in percentages. In experiment 2, the contrast of the inducers was set to different maximum contrasts for each photoreceptor due to constraints of the silent substitution method and differences in thresholds (Figure 4). To highlight these differences between experiments 1 and 2, we used a different notation in experiment 2 (normalization equals to 1) to quantify the effect.